CCC Annual Report

UIUC, August 14, 2013

Effect of Double-Ruler EMBr on Transient Mold Flow with LES Modeling and Scaling Laws

Ramnik Singh
(MSME Student)

Work performed under NSF Grant CMMI 11-30882

Department of Mechanical Science & Engineering
University of Illinois at Urbana-Champaign

Acknowledgments

- National Science Foundation Grant CMMI-11-30882
- Continuous Casting Consortium Members (ABB, ArcelorMittal, Baosteel, Magnesita Refractories, Nippon Steel and Sumitomo Metal Corp., Nucor Steel, Postech/ Posco, Severstal, SSAB, Tata Steel, ANSYS/ Fluent)
- Mr. Jonathan Powers and Mr. Thomas Henry, Severstal, Dearborn, MI.

Outline

Previous work with CUFLOW

- validated with measurements in a scaled caster in presence of conducting-side walls and ruler-EMBr
- used to understand the effects of wall conductivity in detail.

These results are in 2012 CCC annual meeting and reports

Recent findings:

Part I

- Evaluate scale-up criteria from a scaled physical model to the real caster, including presence of applied magnetic field.

Part II

- Investigate transient turbulent flow in a real commercial caster with / without double-ruler EMBr field;
- validate with nail board measurements.

Overview: Governing equations for Incompressible MHD flow for low magnetic Reynolds number(Re_M)

Fluid Flow Equations

1. Mass conservation $$\frac{\partial v_j}{\partial x_j} = 0$$

2. Momentum conservation $$\frac{\partial v_i}{\partial t} + \frac{\partial v_i v_j}{\partial x_j} = -\frac{1}{\rho}\frac{\partial p^*}{\partial x_i} + \frac{\partial}{\partial x_j}\left((\nu_0 + \nu_{sgs})\left(\frac{\partial v_i}{\partial x_j} + \frac{\partial v_j}{\partial x_i}\right)\right) + \frac{1}{\rho}F_i$$

MHD Equations- Electric potential method

3. Charge conservation $$\nabla \cdot \vec{J} = 0$$

4. Current density (Derived using Ohm's law with assumption that Re_M<<1 for liquid metal flows) $$\vec{J} = \sigma(-\nabla\varphi + \vec{v} \times \vec{B})$$

5. Poisson equation for electric potential (with variable conductivity) $$\nabla \cdot \sigma\nabla\varphi = \nabla \cdot \sigma(\vec{v} \times \vec{B})$$

6. Lorentz force $$\vec{F} = \vec{J} \times \vec{B}$$

Details of CUFLOW Model

- LES with in-house model, CUFLOW developed by P. Vanka.
- Graphic Processing Unit(GPU) used to perform faster computations.
- Based on Finite Volume Method (FVM).
- Adams-Bashforth scheme applied for time integration.
- Second order central differencing scheme used in space.
- Pressure Poisson and electric Poisson equations solved using a geometric multigrid method.
- Wall-Adapting Local Eddy-viscosity (WALE) and Coherent Structure Model (CSM) sub-grid scale models used.
- Previously validated in several non-magnetic and magnetic flows (Shinn et al. 2013, Chaudhary et al. 2010,2012)

Part I

Details of the Scaled Physical Model

UDV (Ultrasonic Doppler Velocimeter) Probe measurements

Working fluid is a low melting-eutectic alloy (GaInSn)

0.5mm Brass walls placed on wide faces to study effects of wall conductivity

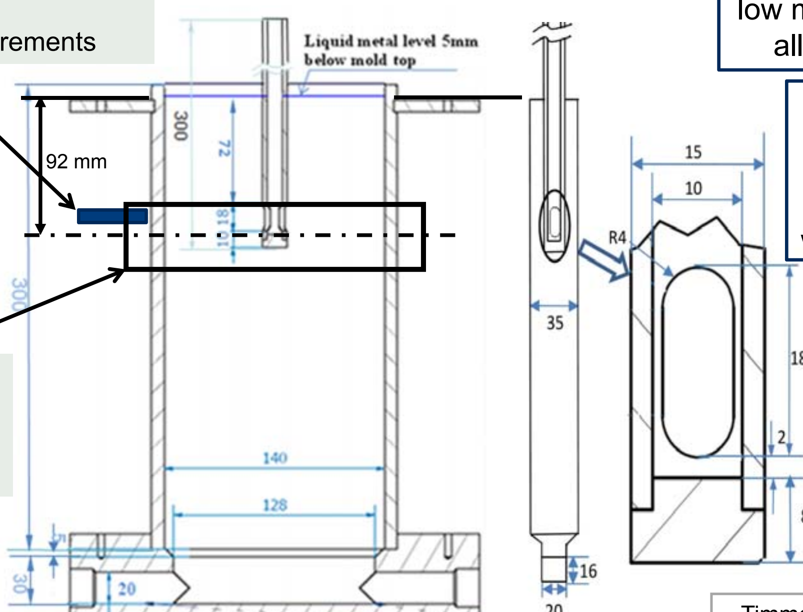

Ruler EMBr 92mm below the Free Surface

Timmel et al. 2011

Details of the Corresponding Real Caster and Applied Ruler EMBr

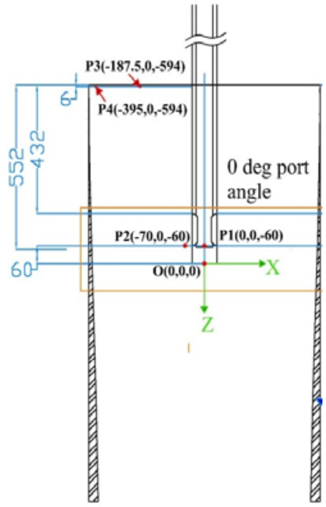

(a) Front- View

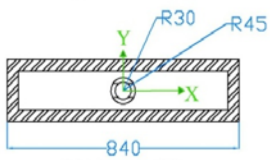

(c) Bottom-View

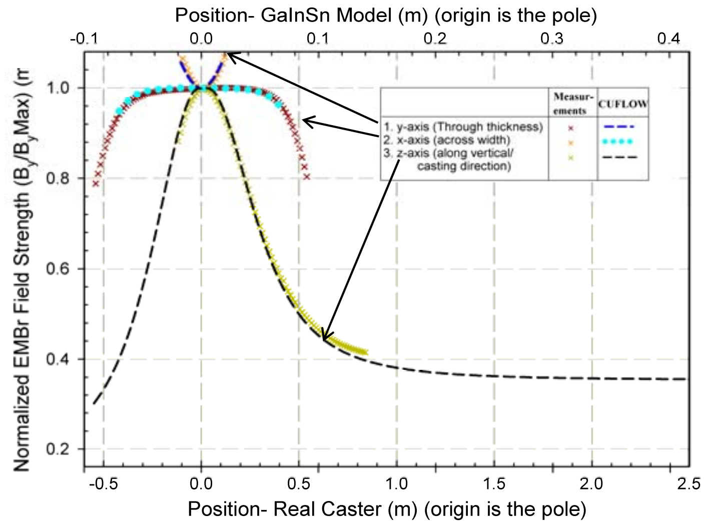

nes
e
el.

Pole is located 92mm and 552mm below free surface for GaInSn model and Real caster respectively (B_yMax= 0.31Tesla)

Measurements (Timmel et al. 2012, 2010)

7

Computational Domains and Boundary Conditions

	GaInSn Model	Real Caster
Number of mesh points	7.6 million	8.8 million
Mold width	140mm	840mm
Mold thickness	35mm	210mm
Mold length	330mm	1980mm
Domain length	330mm	3200mm
Nozzle port dimensions$(width \times height)$	8mm×18mm	48mm×108mm
Nozzle bore diameter$(inner\|outer)$	10mm|15mm	60mm|90mm
SEN submergence depth (liquid surface to top of port)	72mm	432mm
Thickness of shell on the wide faces	0.5mm	$s(mm) = 2.75\sqrt{t(s)}$
Thickness of shell on the narrow faces	0mm	$s(mm) = 2.75\sqrt{t(s)}$

Velocity Inlet Boundary: $$V_z(r) = V_z^{centerline}\left(1-\frac{r}{R}\right)^{\frac{1}{7}}$$

Convective Boundary Outlet: $$\frac{\partial u_i}{\partial t} + U_{convective}\frac{\partial u_i}{\partial n} = 0$$

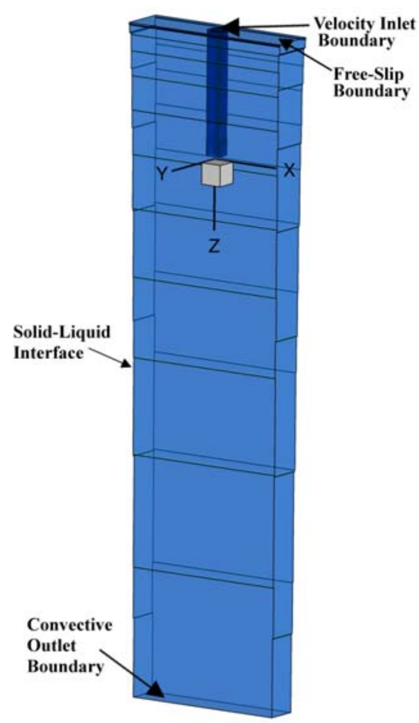

Scaleup Criteria

$$Froude\ Number = \frac{V}{\sqrt{Lg}} = \frac{inertial\ force}{gravitational\ force}$$

$$Stuart\ Number = \frac{B^2 L\sigma}{\rho V} = \frac{Ha^2}{Re} = \frac{electromagnetic\ force}{inertial\ force}$$

Where, V is characteristic velocity (m/s)
B is maximum applied field strength
ρ is material density (kg/m^3)
Re is Reynolds number
L is characteristic length (m)
σ is conductivity of material (1/Ωm)
Ha is Hartmann number

	Stuart Number (based on Mold Width)	Froude Number (based on Mold Width)	Mean Inlet Velocity(m/s)	Casting Speed (m/min)	Magnetic Field Strength B_{max} (mT)	Case (MTB)
GaInSn model (1/6th Scaled Model)	4.84	1.19	1.4	1.35	310	3
Froude Number Similarity	2.49	1.19	3.43	3.3	310	
Stuart Number Similarity	4.84	0.59	1.7	1.64	310	5
Maintaining both Simultaneously	4.84	1.19	3.43	3.3	440	

Evaluation of Stuart Number Scaling

- Velocity field in the GaInSn model is scaled to predicted velocities in the real caster using the relation

$$V_R = V_S\left(\frac{V_{R0}}{V_{S0}}\right) = 1.21 V_s$$

where, S = scaled physical model, R = real caster,
0 = characteristic value (eg at inlet),
L = length, V = velocity

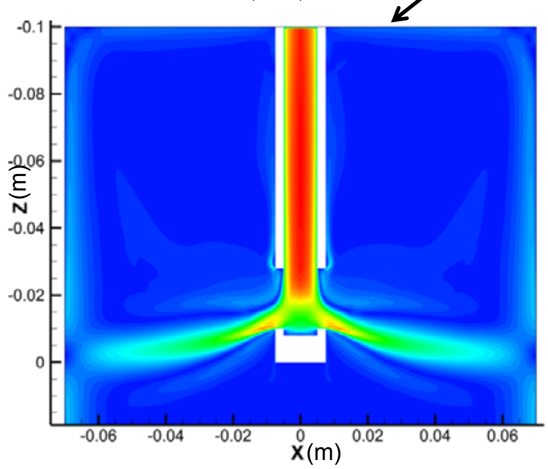

Contours of Scaled Velocity Magnitude for **GaInSn Model** with Conducting Walls.

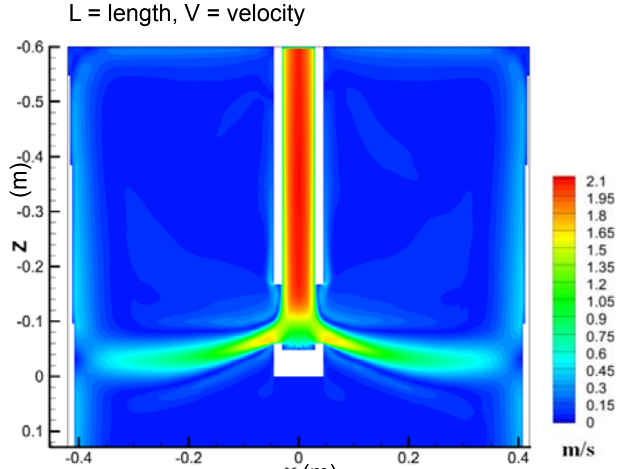

Contours of Velocity Magnitude for **Real Caster** with EMBr

Top Surface velocity across the Mold Width

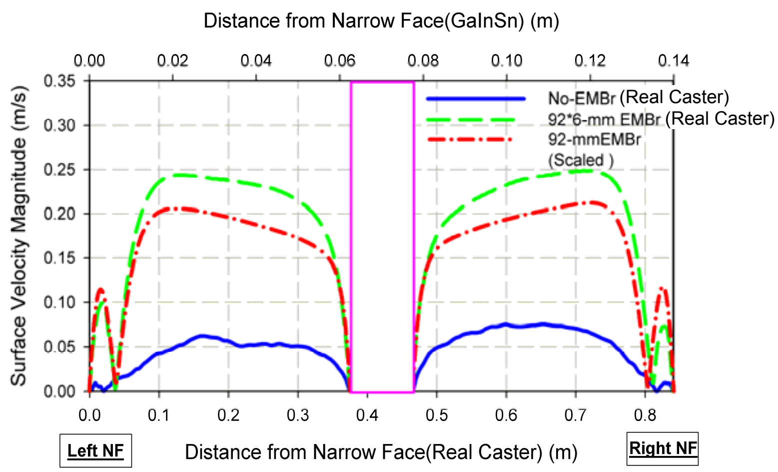

Prediction of real caster from scaled model

- Real caster surface velocity higher than predicted from scaled model caster
- Caused by tapered side walls which push more fluid into the upper recirculation [Chaudhary et al. 2009]

Surface Level Fluctuations

- The obvious scaling method using the length ratio (=6) over predicts the fluctuations in the real size caster.

- General method to predict real caster level fluctuations (Z_R) from scaled model level fluctuations (Z_S) :

$$Z_R = Z_S \frac{Fr_S}{Fr_R}\left(\frac{V_{R0}}{V_{S0}}\right)^2 = Z_S \frac{1.19}{0.59}\left(\frac{1.64}{1.35}\right)^2$$

$$= 2.97\, Z_S$$

- Where *Fr* is the Froude number

$$Fr = \frac{V}{\sqrt{gL}}$$

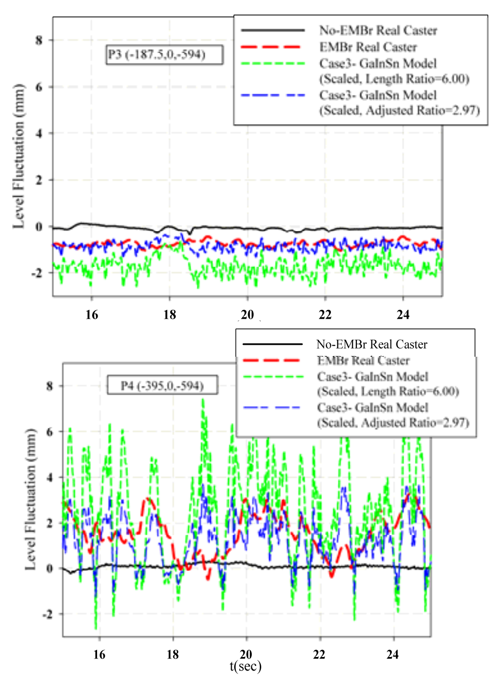

Physical Model Scaling Method with Surface Level Fluctuations

General method to predict real caster **velocities** (V_R) from scaled model velocity (V_S) results:

$$V_R = V_S \left(\frac{V_{R0}}{V_{S0}}\right) \quad \text{Everywhere}$$

S = scaled physical model
R = real caster
0 = characteristic value (eg at inlet)
L = length
V = velocity
Fr = Froude number

$$Fr = \frac{V}{\sqrt{gL}}$$

General method to predict real caster **level fluctuations** (Z_R) from scaled model level fluctuation (Z_S) results:

$$Z_R = Z_S \, \frac{Fr_S}{Fr_R} \left(\frac{V_{R0}}{V_{S0}}\right)^2$$

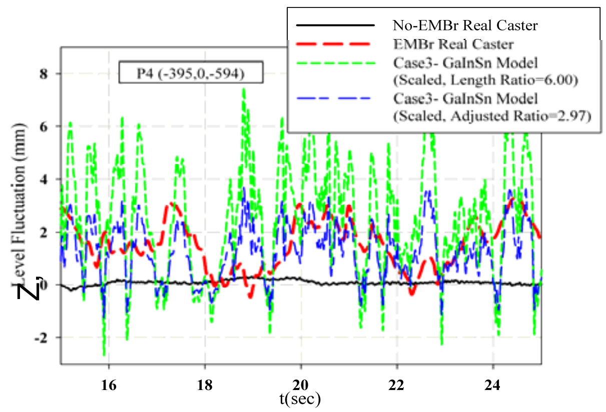

Part I- Conclusions

- The Stuart number similarity criterion enables a close match of both the time-averaged mold flow pattern (qualitative) and velocities (quantitative).
- Simply scaling the surface-level fluctuations using the geometric scale factor (=6) resulted in an overprediction.
- The surface-level fluctuations match well when scaled using a scaling factor based on the ratio of the Froude numbers.
- This new scaling method avoids the need to maintain both the Stuart number and the Froude number simultaneously when choosing the operating conditions for a scaled model caster with EMBr.

Part II

Details of the Commercial Caster

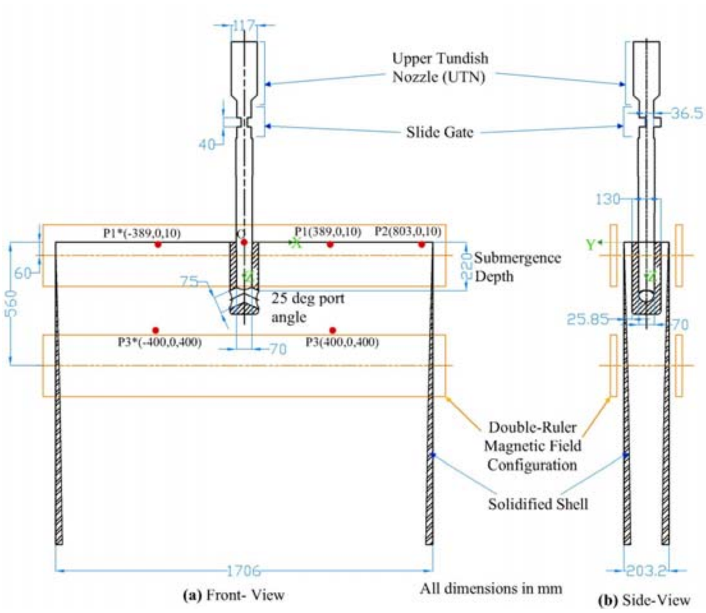

Operating Conditions

Mold width (L)	1706.0 *mm*
Mold thickness	203.2 *mm*
Nozzle port diameter	75.0 *mm*
Nozzle bore diameter (d) $(inner \mid outer)$	70 *mm* | 130 *mm*
Nozzle port angle	25.0 *deg*
Casting speed	1.4 m/min
Slide gate orientation	90.0 *deg*
Slide gate opening fraction (f_A)	41.48%
SEN submergence depth (liquid surface to top of port)	220 *mm*
Total volume flow rate	8.1 *L/s*
Mass flow rate	3.4 tonne/min
Bulk velocity at UTN inlet	0.752 m/s
Bulk velocity at SEN cross section (U)	2.1 m/s
Argon gas injection (volume fraction)	4.37% (ignored)

Shell Profile approximated by
s(mm)=k$\sqrt{t(sec)}$
k= 2.75 mm/$\sqrt{sec}$
Iwasaki et al. 2012

Computational Domain, Mesh and Boundary Conditions

Thickness of shell (uniform around perimeter)	$s(mm) = 2.75\sqrt{t(s)}$
Viscosity (steel)	0.86 x 10^{-6} m^2/s
Fluid density (steel)	7000.0 kg/m^3
Conductivity of liquid (σ_{liquid})	0.714 x 10^6 1/Ωm
Conductivity of walls (σ_{wall})	0.787 x 10^6 1/Ωm
Reynolds number, (Re=Ud_{inner}/ν, based on nozzle diameter)	171,000
Reynolds number, (Re=UL/ν, based on mold width)	41,66,000
Hartmann number (Ha= $BL\sqrt{\sigma/\rho\nu}$, based on mold width)	5,202
Froude number (Fr= $U/\sqrt{gL}$), based on mold width)	0.513
Stuart number (N= $B_0^2 L\sigma/\rho U$), based on mold width)	6.5
Cases	1. No-EMBr 2. With EMBr

Total Number of cells in the mesh= 5.5 million

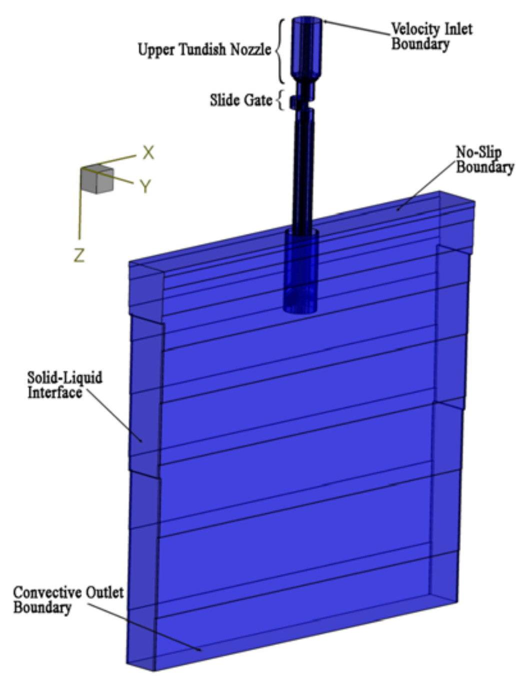

Applied Double Ruler Magnetic Field

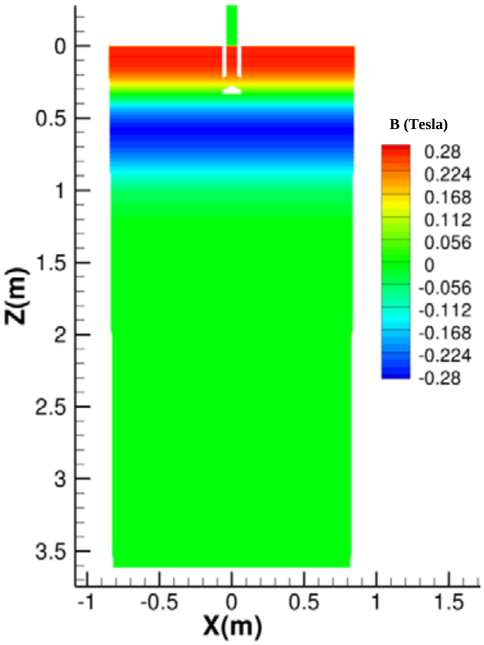

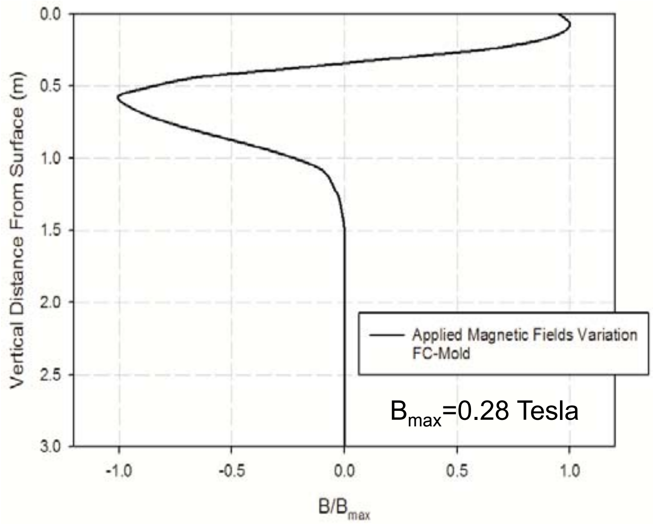

- The magnetic field is adopted from a study by Idogawa et al. 1993

Instantaneous Results

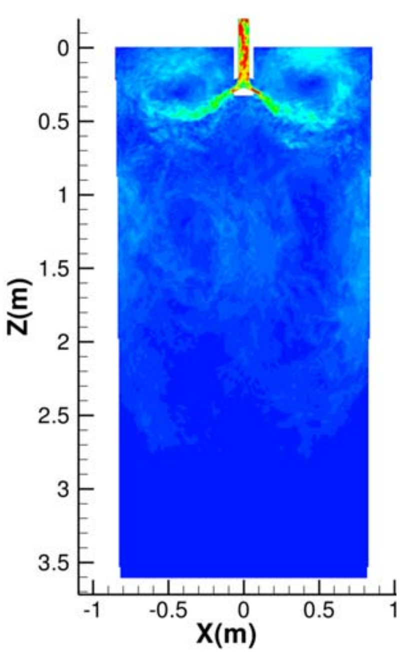

No-EMBr

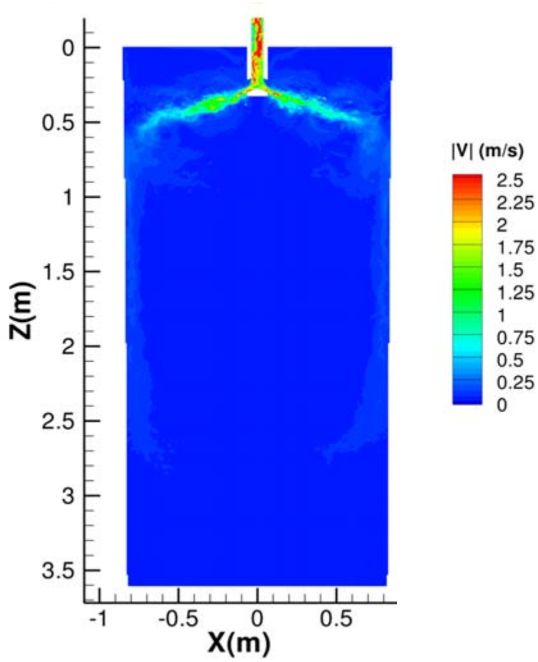

EMBr

Flow stability is aided by conducting solid steel shell

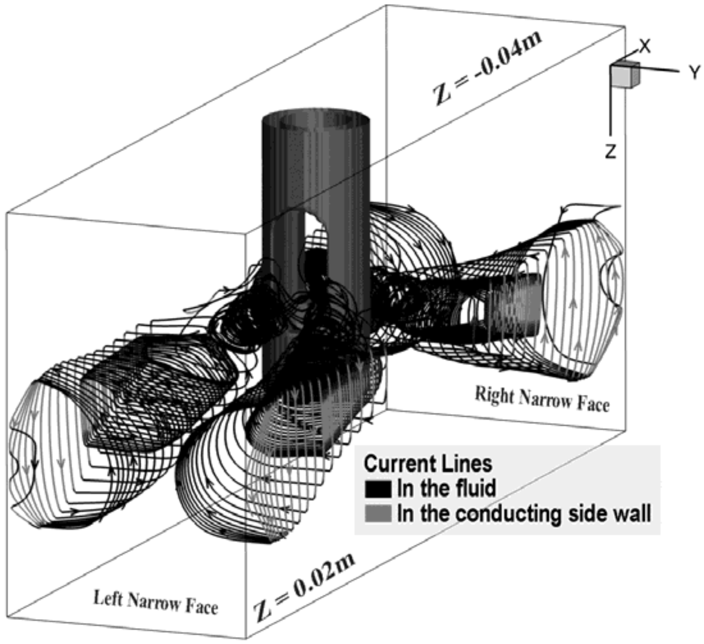

Unbalanced Flow Analysis

No-EMBr **EMBr**

P1- at the top surface

P3- In the jet region

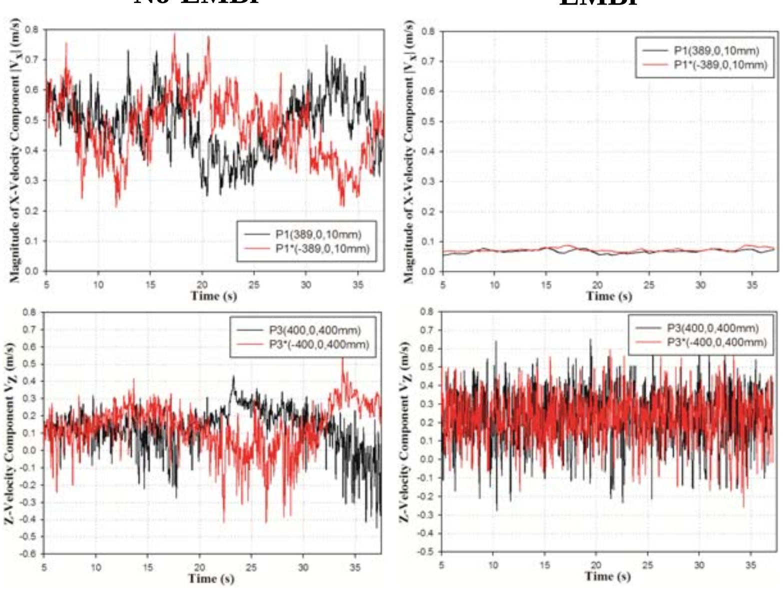

Surface Flow Behavior: Vortex Shedding across the SEN

No-EMBr

EMBr

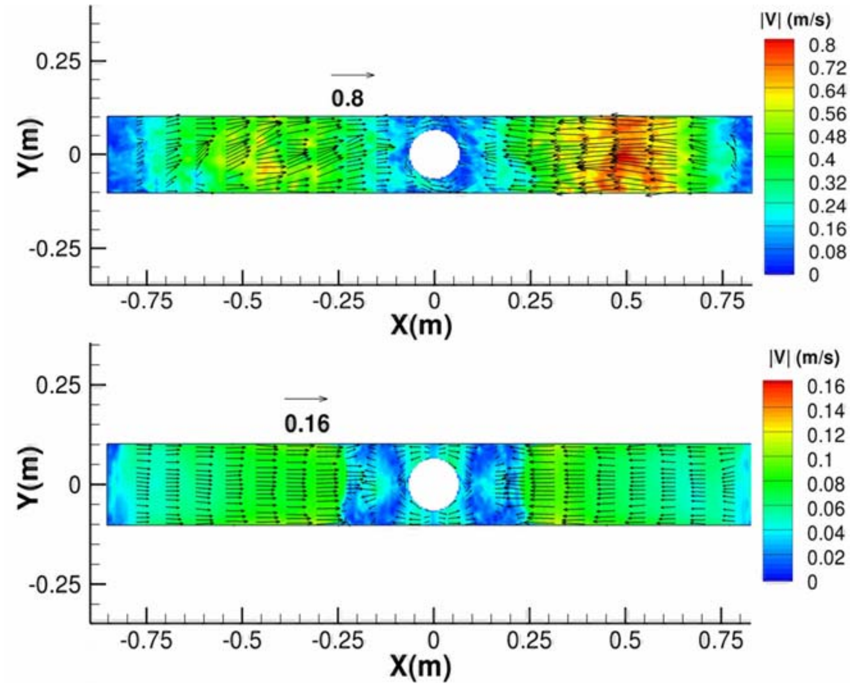

Surface level Profile and Surface Level Fluctuations

No-EMBr

EMBr

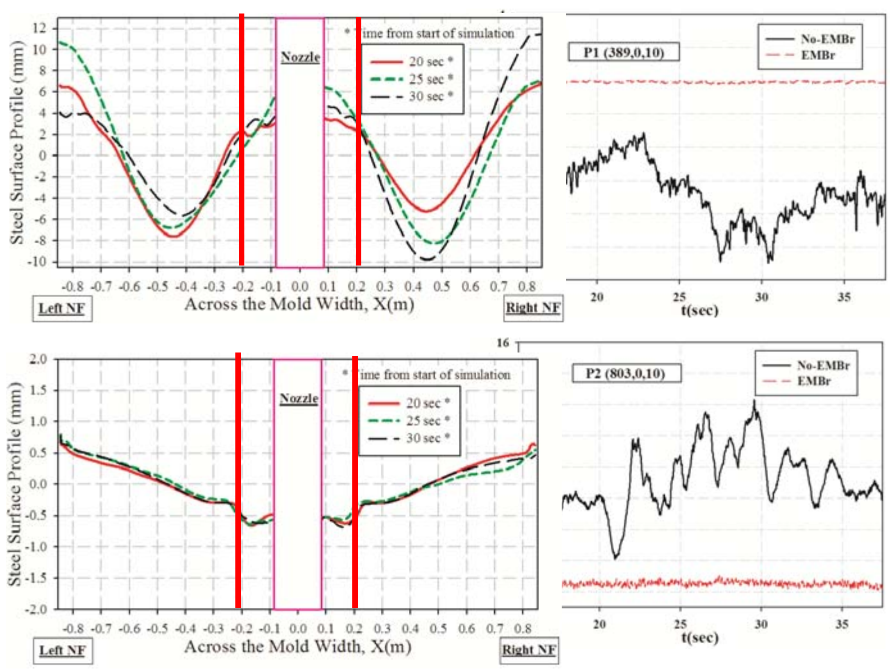

Time-Averaged Results: Nozzle Flow

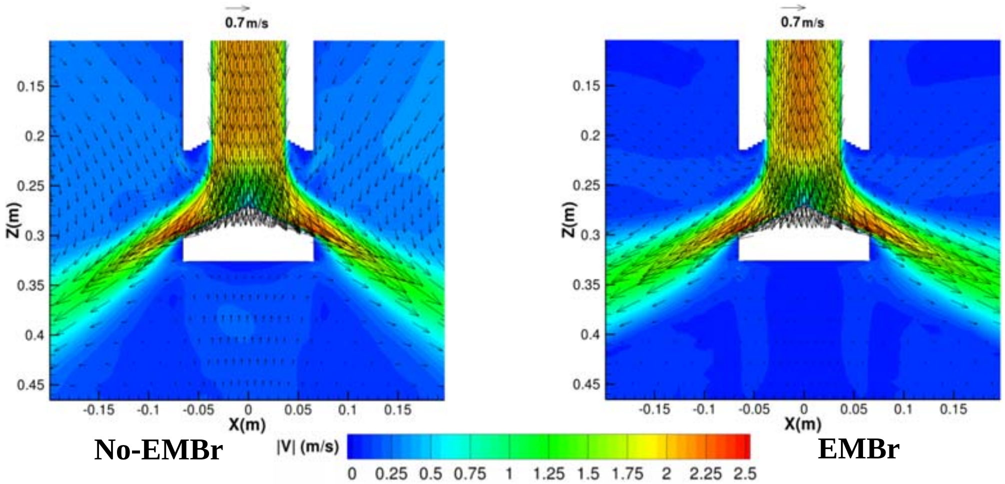

- The mountain-bottom SEN produces thin and strong jets
- Flow inside the SEN ports is similar for both cases as the double-ruler EMBr configuration applies only a low magnetic field in this region

Mold Flow

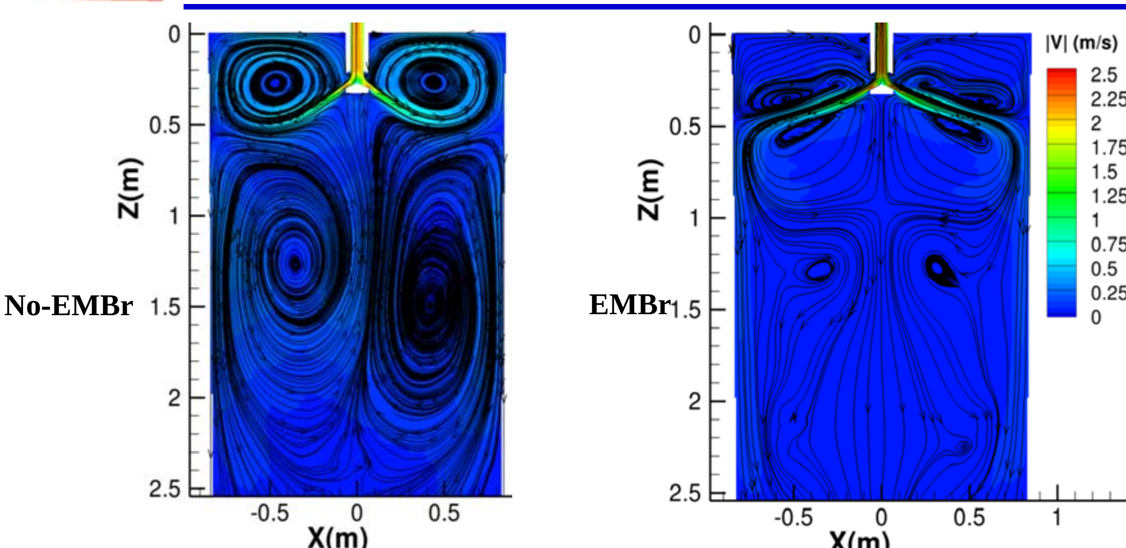

No-EMBr - Exhibits a typical double-roll flow pattern
- Almost symmetric mean flow field after 25 seconds of averaging with slight asymmetry in the lower roll indicating long-time transients

EMBr - Complicated flowfield with lower velocities in upper and lower rolls

Vertical Velocity Below Jet Region

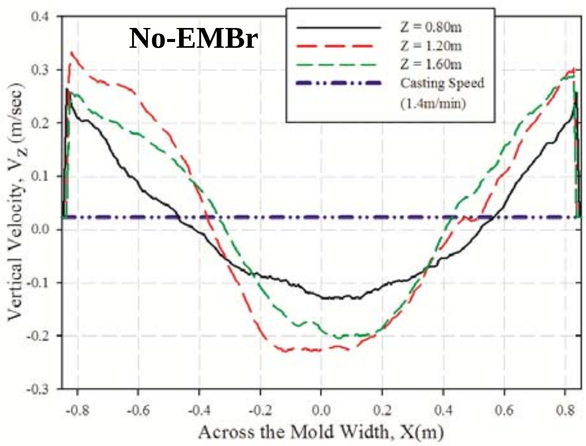

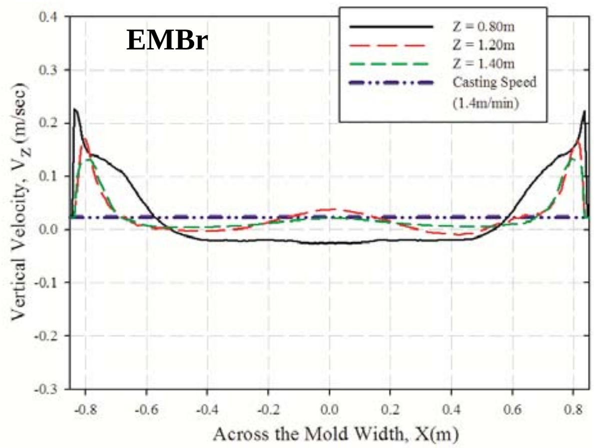

No-EMBr - High downward near the NF and returning flow up the center
- Downward velocity near the NF remains high even at 1.6m from the free surface

EMBr - Has slower downward flow near the NF, which decreases with distance below the top surface

Top Surface Velocity

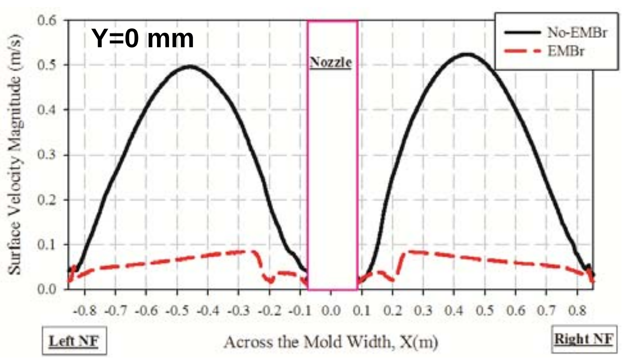

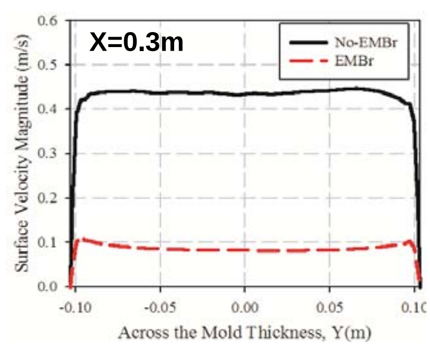

No-EMBr - High surface velocity with the maximum (~0.55 m/s) found midway between the SEN and the NF
- Constant velocity through the thickness

EMBr - Much smaller surface velocities
- Through thickness has a slight M-Shaped profile

Nail Board Measurement

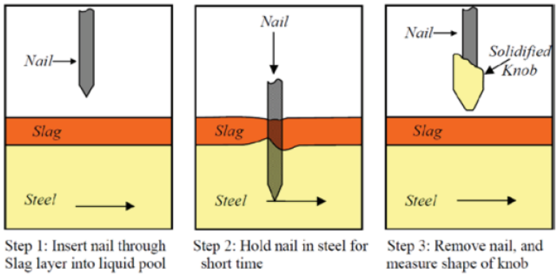

Nail Board Test Procedure [Cukierski and Thomas 2008]

Pictures of one of the nail board used for the measurements

Surface velocity V_{lump} (m/s) calculated using the the lump height difference Δh_{lump} (mm) and the lump diameter d_{lump} (mm) according to the correlation proposed by Liu et al. 2011

$$V_{lump} = 0.624\,(d_{lump})^{-0.696}\,(\Delta h_{lump})^{0.567}$$

Comparison with Nail Board Measurements Top surface Velocity

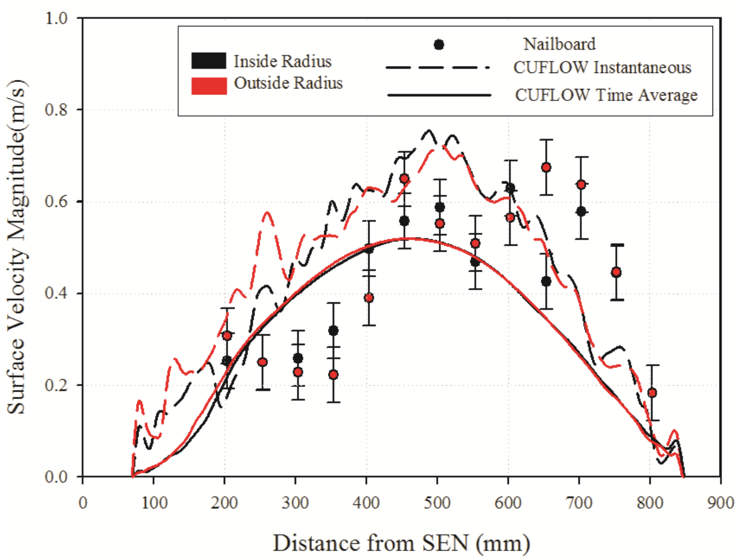

- Measured velocity high near NF.
- Calculated velocity maximum midway between the NF and SEN.
- Maximum of measured velocity quantitatively match the calculated velocity during the phase with stronger surface flow

Top Surface Level Profile

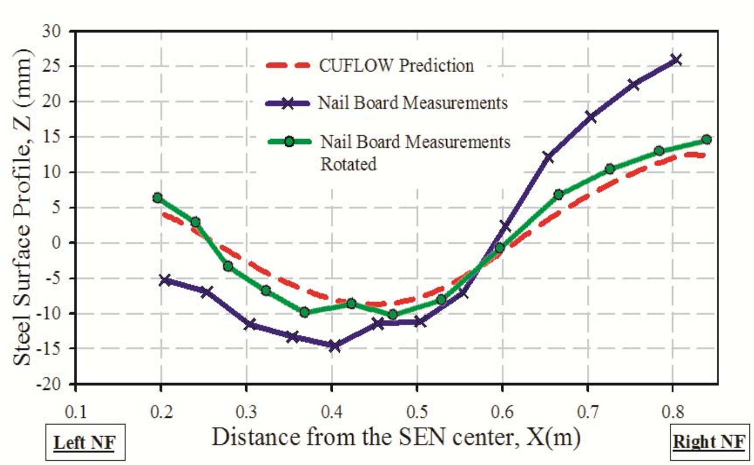

- The measured and the predicted surface level match very closely if the measured profile is rotated.
- This error could easily have been introduced while dipping the nail board manually into the mold

Part II- Conclusions

- The measured surface flow directions, velocity profile, and the free surface level profile all agree reasonably well with the computations.
- Without EMBr, upper recirculation regions have high velocities causing:
  - large variations in surface level profile, (up to ~22mm),
  - large surface level fluctuations (~ +/- 12mm)
  - high surface velocities (up to ~0.6m/s).
- With EMBr, jet is deflected downwards, which
  - weakens upper recirculation regions,
  - flatter surface level profile (up to ~1.5mm),
  - extremely small level fluctuations (< +/- 1mm)
  - lower surface velocities (<0.1m/s).
- The application of this EMBr field also damps the unbalanced flow behavior and makes flow much more stable.

Recommendations

- Conduct plant trials to investigate steel quality to confirm flow issues of greatest importance is excessive surface flow
- Use computational models to predict behavior of EMBr before installing
- Measure magnetic field to check uniformity across mold width. (If field strength weakens towards NF, may need higher EMBr strength)
- May also need to adjust EMBr strength according to submergence depth and casting speed / mold width (in addition to nozzle geometry)
- For caster studied here:
  Use double-ruler EMBr (FC-mold) with half strength on upper field
  - This should slow down and stabilize surface flow
  - And lessen particle entrainment deep into caster

References

1. K. Timmel, S. Eckert, G. Gerbeth, Experimental investigation of the flow in a continuous-casting mold under the influence of a transverse, direct current magnetic field, Metall. Mat. Trans. B, DOI: 10.1007/s11663-010-9458-1.
2. R. Chaudhary, B. G. Thomas, S. P. Vanka, Effect of electromagnetic ruler Braking (EMBr) on transient turbulent flow in continuous slab casting using large eddy simulations, Metall. Mat. Trans. B, DOI: 10.1007/s11663-012-9634-6.
3. X. Miao, K. Timmel, D. Lucas, Z. Ren, S. Eckert, G. Gerbeth, Effect of an electromagnetic brake on the turbulent melt flow in a continuous-casting mold, Metall. Mat. Trans. B, DOI: 10.1007/s11663-012-9472-0.
4. R. Chaudhary, A. F. Shinn, S.P. Vanka, B.G. Thomas, Direct numerical simulations of transverse and spanwise magnetic field effect on turbulent flow in a 2:1 aspect ratio rectangular duct, Computers and Fluids, DOI: 10.1016/j.compfluids.2011.08.002.
5. A. Idogawa, M. Sugizawa, S. Takeuchi, K. Sorimachi, and T. Fujii., “Control of molten steel flow in continuous casting mold by two static magnetic fields imposed on whole width.”, Materials Science and Engineering: A, 1993, vol. 173, pp. 293-297.
6. R. Singh, B.G. Thomas, and P. Vanka, “Effects of a Magnetic Field on Turbulent Flow in the Mold Region of a Steel Caster,” Metallurgical and Materials Transactions B, in press.
7. R. Singh, B.G. Thomas and S.P. Vanka, “Large Eddy Simulations of Effect of Double-Ruler Electromagnetic Field on Transient Flow during Continuous Casting”, CCC Report, 2013